Ocean Engineering 130 (2017) 166–175

Contents lists available at ScienceDirect

Ocean Engineering

journal homepage: www.elsevier.com/locate/oceaneng

On-board measurement techniques to quantify underwater radiated noise level

Serkan Turkmen*, Batuhan Aktas, Mehmet Atlar, Noriyuki Sasaki, Rod Sampson, Weichao Shi

School of Marine Science & Technology, Newcastle University, Armstrong Building, NE1 7RU United Kingdom

ARTICLE INFO

Keywords:
Underwater radiated noise
Propeller cavitation
Full scale measurements
Correlation method
SONIC project

ABSTRACT

Cavitating ship propellers are known to be the dominant noise source contributing significantly to the underwater radiated noise (URN) level. Innovative measurement methods using on-board devices need to be further investigated as they offer a serious alternative to traditional methods in terms of cost-efficiency and practicality. This exploratory study combined simultaneous on- and off-board noise and vibration measurements with cavitation views captured by digital photography and high speed cameras.Comprehensive full-scale trials were conducted on Newcastle University's research vessel, The Princess Royal, in the framework of the FP7-EU project SONIC. On-board data were captured from multiple measurement systems (including. hull pressure sensors, accelerometers, optical devices, shaft strain gauges) provided by SONIC project partners CETENA, Wärtsilä , University of Southampton and Newcastle University. A new semi-empirical correlation method based on cavitating propeller pressure fluctuation and the URN level was established. Results offer clear evidence of successfully estimating URN with on-board measurements up to the middle frequency region where the blade passing fundamental and low harmonic frequencies occur. These illuminating insights reported in this paper provide valuable benchmark sea trial data in full scale.

1. Introduction

Quantifying the underwater radiated noise (URN) of ships is not a simple process because ships are installed with many types of machinery, causing different noise and vibration levels. URN can be generated mechanically by on-board reciprocating engines, machinery as well as hydrodynamically e.g. mainly due to their propeller(s) (Fischer and Brown, 2005; ITTC, 2014). During the combustion process, high gas pressure forces and inertial forces excite the system to vibrate and generate structure borne noise in the firing rate harmonics (Vorus, 1988; Arveson and Vendittis, 2000). The overall URN level of surface ships can be associated with vessel speed and displacement up to 100 Hz for commercial vessels (Ross, 1976). Noise generated by non-cavitating propellers can be divided into two categories; the first one is low frequency blade rate noise induced pressure fluctuations, and the other is high frequency broadband cavitation noise (e.g. Urick, 1967, Carlton, 2012). Fig. 1 shows an idealized non-cavitating propeller noise spectrum. However, URN can be contributed and dominated by propeller blades, especially when cavitation occurs (e.g. Sasajima et al., 1986). Cavitating propellers have more complex noise spectra with considerably higher sound pressure levels than the noise spectra for non-cavitating propellers. Fig. 2 presents the general noise spectrum of cavitating ship propellers (Nilsson and Tyvand, 1981). The blade rate noise through its harmonics can be predicted up to the middle frequency range due to the relatively steady nature of the developed cavitation on the propeller blades (Wales and Heitmeyer, 2002).

Most of the tools to predict URN level and pressure pulses induced by cavitating propellers can be performed for lower frequency by taking into account the propeller geometry, boundary condition, area of sheet cavitation on the propeller blade (Szantyr, 1985; Kinnas et al., 2003; Ekinci et al., 2010). Many unsteady phenomena are involved in the developed cavitation including cavity collapse and shock waves as reported in (Wenz, 1962; Nilsson and Tyvand, 1981; Sasajima et al., 1986, Hallander and Göran 2002). Therefore, predictions get harder beyond the middle frequency range.

In assessing the most accurate levels of the ship's URN full-scale measurements through dedicated noise trials are essential. Full-scale trials involve on-board and off-board measurement devices e.g. hydrophone arrays, accelerometers, pressure sensors and GPS sensors (e.g. Brooker, Humphrey, 2014). Trials using these systems are often complex, expensive and time-consuming to undertake. Moreover, self-noise of the deployed equipment might be apparent in the URN spectra. The distance between the noise source and hydrophones

* Corresponding author.
E-mail address: serkan.turkmen@ncl.ac.uk (S. Turkmen).

http://dx.doi.org/10.1016/j.oceaneng.2016.11.070
Received 19 December 2015; Received in revised form 4 July 2016; Accepted 29 November 2016

Nomenclature

A_o	The propeller disc area
A_E	The expanded area of the blades
AE/Ao	Expanded Blade Area Ratio
D	Diameter [m]
J	Advance Coefficient
N	Rotational speed [rpm]
P/D	Pitch Ratio at 0.7 R
P_D	Delivered power
Q	Torque [Nm]
R	Radius [m]
RL	Received Noise Level
RNL	Radiated Noise levels
SPL	received sound pressure level
SPL′	The level of net sound pressure of the propeller
SPL_n	the background sound pressure level measured (in dB; re 1μPa)
SPL_{s+n}	The total sound pressure level (in dB; re 1μPa)
T	Thrust [N]
V_a	Speed of advance [m/s]
Z	Number of Blades
r_i	Distance between the acoustic center of the target vessel and hydrophone i
r_{ref}	the reference distance (1 m)
μ	Viscosity of the fluid [kg/ms](sea)
ρ	Density of the fluid [ton/m3](sea)
ΔP_z	the total amplitude of pressure fluctuations
ΔP_0	the pressure fluctuation due to the non cavitating propeller
ΔP_c	the pressure fluctuation due to the cavitating propeller
φ	the phase angle

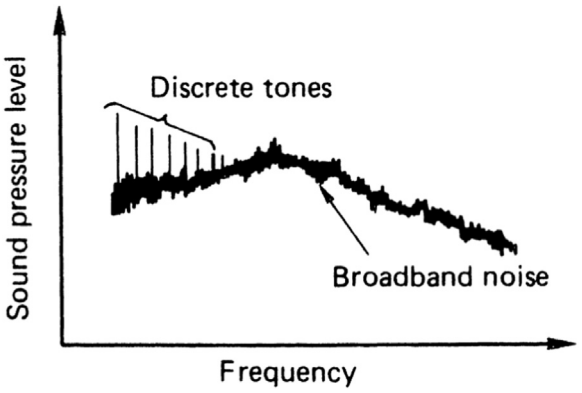

Fig. 1. Non-cavitating noise spectrum (Reproduced from Carlton 2012).

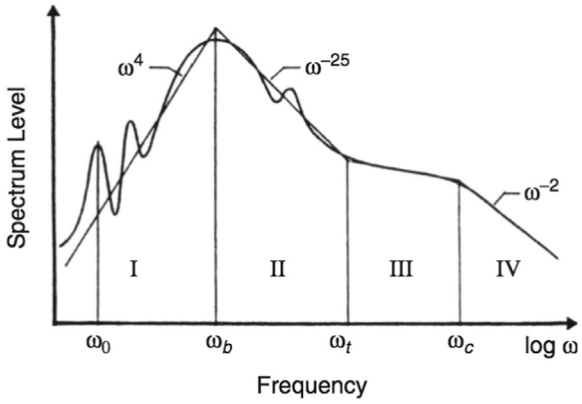

Fig. 2. General noise spectrum level of a cavitating propeller (Reproduced from Nilsson

Fig. 3. The target vessel: Research Vessel *The Princess Royal* (Atlar et al., 2013).

Table 1
Specification of the target vessel RV Princess Royal.

Classification	MCA Cat 2
Overall length	18.9 m
Beam (Full)	7.3 m
Design draft	at AP: 1.96 m at FP: 1.76 m
Displacement (Loaded arrival)	42 t (approx.)
Payload	5 t
Max speed	20 knots
Cruising speed	15 knots
Engines	2 × 602 BHP
Gearbox reduction ratio	1.75
Propulsion	2 × 5-bladed, fixed pitch propellers

cannot be hold constant due to the target vessel continuously moving without employing the rudders. Therefore, a measurement time span (Data Window Period) is necessary for averaging the measured data (ANSI, 2009). Traditional methods offer a high accuracy level to determine the underwater noise generated by shipping. However, cost-effective and hands-on methods of ship noise monitoring need to be investigated.

This paper presents a new method to quantify the URN of a ship by using cost- and time-effective on-board measurement devices. Comprehensive full-scale trials were conducted on The Princess Royal, which is Newcastle University's catamaran type research vessel and the results were analysed and discussed as part of the FP7-EU project called SONIC, Suppression Of underwater Noise Induced by Cavitation (SONIC, 2012). During these trials, an extensive amount of on-board data were captured from multiple measurement systems using hull pressure sensors, accelerometers, ultrasonic transducers, optical devices, etc. Simultaneous off-board radiated noise measurements were also undertaken to establish a correlation between the on-board and off-board noise data. Moreover, the cavitation views were recorded by using digital photography and high-speed cameras to describe the type of the cavitation present on the propellers. Finally, the direct relation between the sound pressure levels measured in the far-field and the dynamics created by the propellers and machinery were investigated.

A general description of the trials, including the Princess Royal as the benchmark vessel and on-board and off-board measurement devices as well as the location of the trial area, is given in Section 2. The full-scale cavitation observations made on-board of the vessel and its major contribution to URN are shown in Section 3. This is followed by a description of on-board and off-board measurement data and their analysis methods in Section 4. A correlation method that was created in this study is presented in Section 5. A conclusion and discussion with a specific emphasis on the correlation study are reported in Section 6.

Table 2
Specification of the propellers (Atlar et al., 2013).

Diameter, D	0.75 m
Pitch Ratio at 0.7 R, P/D	0.85
Expanded Blade Area Ratio, A_E/A_o	1.06
Number of Blades, Z	5
Rake angle	0°
Skew angle	19°
Direction of rotation	Outward
Design Advance Coefficient, J	0.5
Material	NiAlBr

2. Methodology

On-board measurements were carried out to give an indication of the impact of cavitating ship propellers on the underwater noise emission from a catamaran research vessel. A total of 76 runs were completed during the trial. Of these, off-board radiated noise data was recorded on 49 runs. The measurements were undertaken in the region of Northumberland, about 28 km offshore east of Blyth, in the North East coast of England. Water depth in the trials area varies from about 90–100 m at Lowest Astronomical Tide (LAT). Sediment conditions consist of soft mud. The target vessel used in the trials was the RV Princess Royal (Fig. 3), designed, owned and operated by Newcastle University (Atlar et al., 2013). The outline specification of the vessel is shown in Table 1 while those of her propellers are given in Table 2.

Off-board measurements were carried out with deployed hydrophone arrays to record the URN. The array also consists of three hydrophones attached to a central weighted line and a multichannel acquisition system on-board the support vessel. The deployment depths of the hydrophones on the central line are 10, 25 and45m from the water surface. On-board sensors were installed to measure the underwater pressure pulses, hull and engine vibration, engine room sound pressure levels and underwater ultrasonic noise. Off-board measurements were carried out simultaneously for a more conclusive analysis of URN in combination with on-board measurements. GPS data was provided to improve accuracy of the measurement window and time. A range of cameras were used in order to cover as many possibilities and opportunities to capture dynamics of the cavitation. A summary of the sensors deployed by each SONIC project partner is provided in Table 3. The technical details of on-board sensors and Camera Specifications are given in Table 4. The sensors were connected to the Data Acquisition Hardware multi-channel NI CDAQ Chassis with Modules. A laptop were used to log the measured data.

These sensors were complemented by optical observations made through the side by side above each propeller at each demi-hull (shown in Fig. 4), four windows in total, and borescope. Six pressure sensors were used during the trial. The locations were defined to receive the influence of cavitation dynamics on pressure fluctuations above the propeller and in the downstream. Mainly the port side sensors were analysed in this study and Fig. 5 shows the hull locations of the pressure sensors, accelerometers and the windows. The Perspex window does not allow to locate a sensor above the propeller. Therefore the pressure transducers PP2 and PP3, were installed 0.15D behind the propeller disc (D is the propeller diameter) to capture the pressure pulses above the propeller. The transducer PP4 was installed 0.8D behind the propeller disc to capture the pressure pulses in the downstream.

The trials were mainly performed for 4 different operating conditions with main engine speeds of 600, 900, 1200, and 2000 rpm set on the research vessel. The averaged, engine delivered power correspond-

Table 3
The summary of on-board sensors.

Contributing SONIC partner	Port side	Starboard side
Wartsila	1 x engine body accelerometer 1 x hull pressure pulse sensor	1 x engine body accelerometer 1 x engine foundation accelerometer 1 x hull pressure pulse sensor
	1 x hull accelerometer 1 x engine room microphone	1 x engine room microphone
CETENA	2 x hull pressure pulse sensor 1 x shaft speed sensor 1 x engine power sensor 1 x propeller shaft torque sensor 1 x borescope	
Newcastle University		2 x hull pressure pulse sensor 2 x hull accelerometer 4 x cavitation observation cameras
Southampton University (SOTON)	1 x ultrasonic transducer	

Table. 4
The technical details of on-board sensors.

Sensor	Sensor description	Frequency sampling
Pressure Transducer 1	XPM10 Miniature pressure sensor	2 kHz
Pressure Transducer 2	XPM10 Miniature pressure sensor	2 kHz
Accelerometer 1	Wilcoxon Model 797 V Low profile, IsoRing® PiezoVelocity	2 kHz
Accelerometer 2	Wilcoxon Model 797 V Low profile, IsoRing® PiezoVelocity	2 kHz
Torque	Single-channel torque measurement via strain gauges (full bridge)	565 samples/second
Thrust	Single-channel axial load (thrust) measurement via strain gauges (full bridge)	565 samples/second
RPM	Once-per-rev pulse measurement	565 samples/second
High Speed Camera (starboard side)	Nanosense Mark 3	2000 fps
Digital camera (portside)	Digital camera 240 FPS Samsung Galaxy	Stationary picture, 120 fps
Digital Camera (port side)	Digital Camera 240 FPS GoPro	Stationary picture, 240 fps
Digital Camera (port/ starboard side)	Nikon D700 + 20 mm f2.8 lens	6400 ASA giving 1/1000 s at f 2.8 still images

Fig. 4. Portside (Perspex Windows) above the propeller.

ing to the operational conditions is given in Table 5.

3. Cavitation observation

Since the type, extent, volume, density and dynamics of the cavitation play a major role in contributing to the URN levels this section summarizes the cavitation observations made on-board the vessel through the portholes (Perspex Windows) above her propellers as shown in Fig. 4. Some pictures were taken from outer side windows some from inner side windows. The full documentation of the cavitation observations during the SONIC noise trials can be found in Sampson et al. (2015). The vessel's lowest engine speed is 600 rpm. At this speed, as shown in Fig. 6, no cavitation was visible. In fact, the inception of the tip vortex was between 650 and 700 engine rpm.

When the vessel was operated at an engine speed of 900 rpm

Table 5
Full-Scale Average Running Conditions.

Engine		Propeller N	P_D	P_D
[RPM]	Torque [kNm]	[rpm]	[kW]	[%MCR]
600	0.3	342.8	10	2.22
900	0.6	514	31	6.89
1200	1	679.5	71.6	15.91
2000	2.77	1141.5	329.3	73.18

cavitation could be observed on the propeller. The dynamics of the cavitation at this speed can be described as less intermittent, rather continuous "stable leading edge vortex cavitation" emanating from the suction side of the blade and continuing in the slipstream as a trailing vortex extending to the rudder. This is supported by the picture shown in Fig. 7.

Fig. 8 shows the nature of cavitation at the 1200 rpm engine speed. At this speed cavitation is characterized as a strong suction side "Sheet Cavitation" emanating from the entire blade leading edge with increased extent (hub to tip) terminating the blade by rolling-up in the form of "Trailing Tip Vortex" extending to the rudder. Partial "break-up" of the sheet cavitation as well as occasional appearance of intermittent "Hub Vortex Cavitation" (in Fig. 9) and "Hull-Propeller Vortex" cavitation were observed.

Fig. 10 shows the cavitation pattern observed at the maximum engine speed of the vessel, 2000 rpm. At this speed, the extent of sheet cavitation is the largest covering almost 25–30% of the suction side of the blade. The volume of the sheet cavity and its intensity are further increased. As far as the cavity dynamics is concerned, the sheet

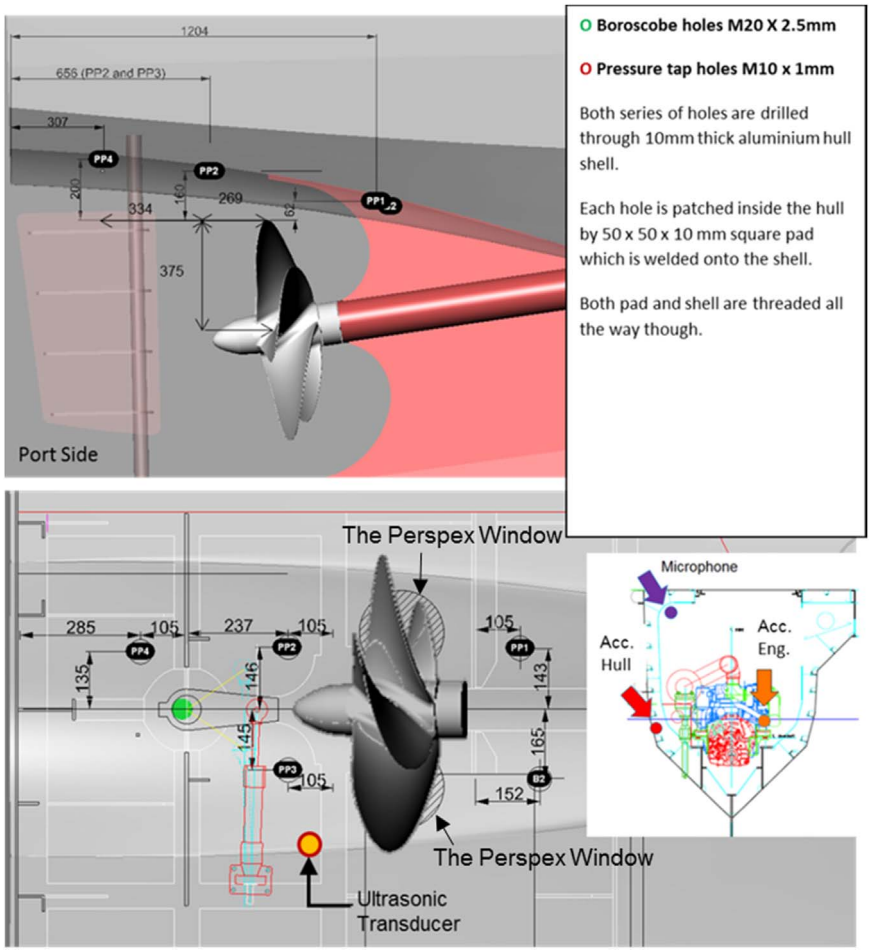

Fig. 5. Port side sensor hole arrangement of The Princess Royal for the first trial.

Fig. 6. Full-scale trial cavitation observation – 600 engine rpm.

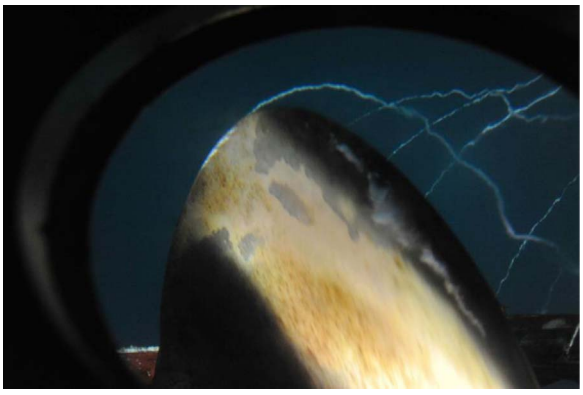

Fig. 7. Full scale trial cavitation observation– 900 engine rpm.

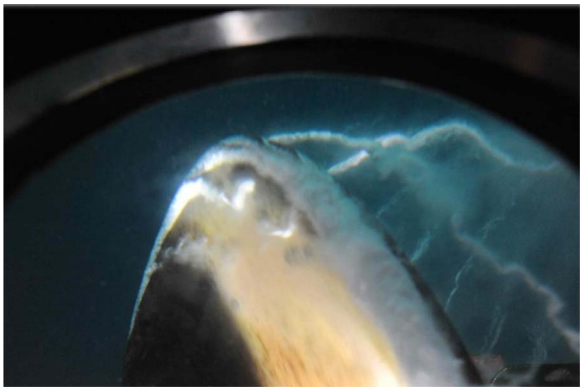

Fig. 8. Full scale trial cavitation observation – 1200 engine rpm.

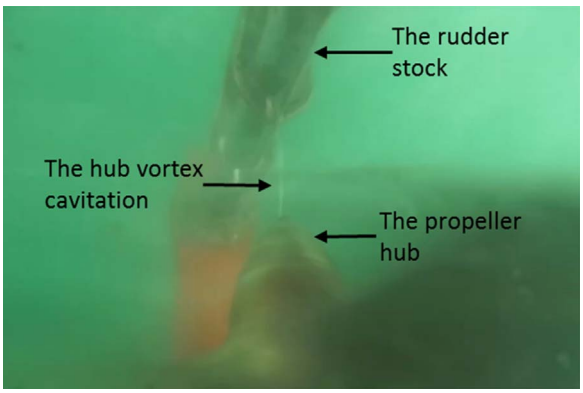

Fig. 9. The hub vortex cavitation (captured from the footage)– 1200 engine rpm.

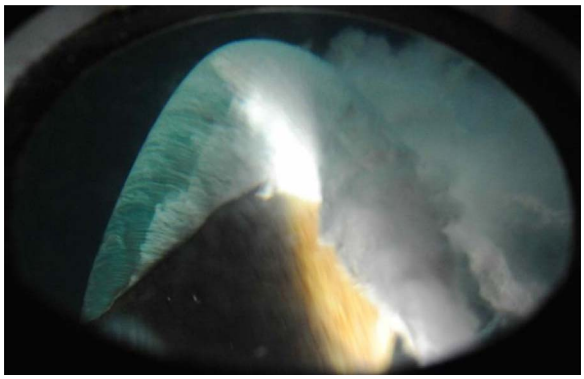

Fig. 10. Full scale trial cavitation observation – 2000 engine rpm.

cavitation is extremely unsteady and breaking-up and bursting, occasionally with a cloudy appearance. This sheet cavitation terminates the blade at tip region by rolling-up, rather thick, intense and cloudy tip vortex and dominating the propeller slipstream up to the rudder. Occasionally this trailing vortex bursts. The left picture in Fig. 11 shows the Hub-Vortex cavitation which is much thicker, intense and continuous. The Hull-Propeller Vortex cavitation very often develops with increased vortex diameter as also shown in Fig. 11 right picture.

4. Results of the on-board and off-board measurements

The off-board radiated noise data were measured by using CETENA's and Southampton University's hydrophone arrays following procedures of ISO/PAS 17028-1: 2012 and ANSI S12.64 (Humphrey et al., 2015). Each array consisted of three digital hydrophones each with a depth sensor. The acquisition system is a multi-channel data receiver that is able to get a continuous flow of digital data simultaneously from all the hydrophones along with data from a GPS antenna. A moored 14 m catamaran support vessel was used to deploy the vertical hydrophone arrays.

Radiated Noise levels (RNL) received at each hydrophone was found from the Power Spectral Density (PSD) for each run within the Data Window Period (in μPa^2. Hz^{-1}). The received PSD level for each hydrophone is provided accordingly in narrowband (NB) spectra (from 4 Hz to 50 kHz) in dB re 1 μPa^2. Hz^{-1}. NB spectra are corrected for range to a reference distance of 1 m to give RNL in dB re 1 μPa^2m^2. Hz^{-1}, by adding the following correction to the averaged received levels

$$RNL = RL + 20\log_{10}\left(\frac{r_i}{r_{ref}}\right) \quad (1)$$

where r_i is the distance between the acoustic center of the target vessel and each hydrophone i at CPA (the slant range) and r_{ref} is the reference distance (1 m). The one-third octave (OTO) band levels in dB re 1 μPa^2m^2 were calculated in the same frequency range as NB spectra and adjusted for the distances between the target vessel and each hydrophone as above. The data were either analysed using real time OTO filters or Fast Fourier Transform (FFT) analysers in accordance with ANSI/ASA S1.11 (ANSI, 2004).

The ship radiated noise data (both NB and OTO band) were adjusted for background noise again using the standards of ISO/PAS 17028 and ANSI S12.64. If the difference between received level during a target vessel run and background noise level was greater than 10 dB no adjustments to NB spectra and OTO band levels were necessary. If the difference was between 3 dB and 10 dB, background noise was subtracted from the ship radiated noise using the following formula:

$$SPL' = 10\log_{10}[10^{(SPL_{s+n}/10)} - 10^{(SPL_n/10)}] \quad (2)$$

where SPL' is the background noise adjusted received sound pressure level (SPL) from the vessel, SPL_{s+n} is the vessel noise plus background

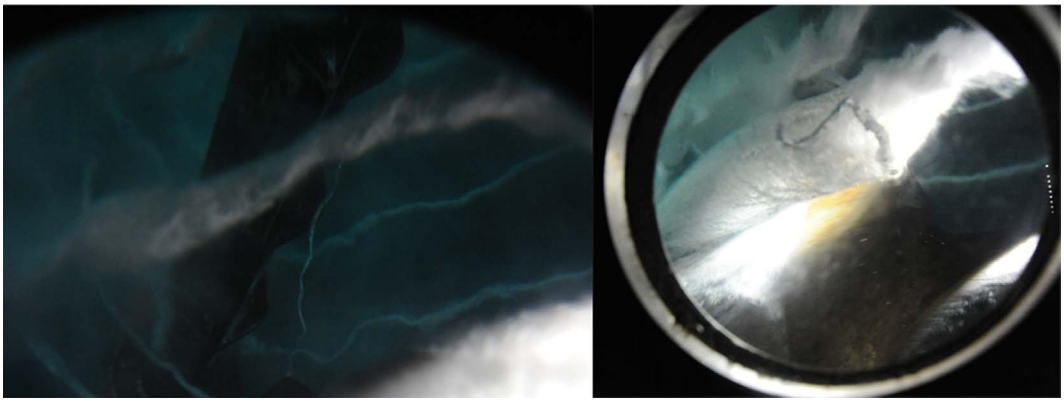

Fig. 11. The hub vortex cavitation (left) and the hull-propeller vortex cavitation (right) – 2000 engine rpm.

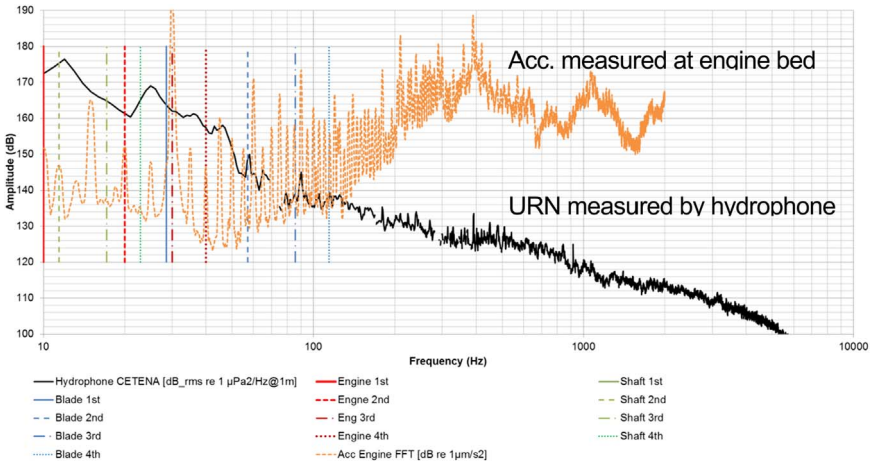

Fig. 12. The main engine acceleration compared with off-board measurements (narrow band) for 600 rpm engine speed.

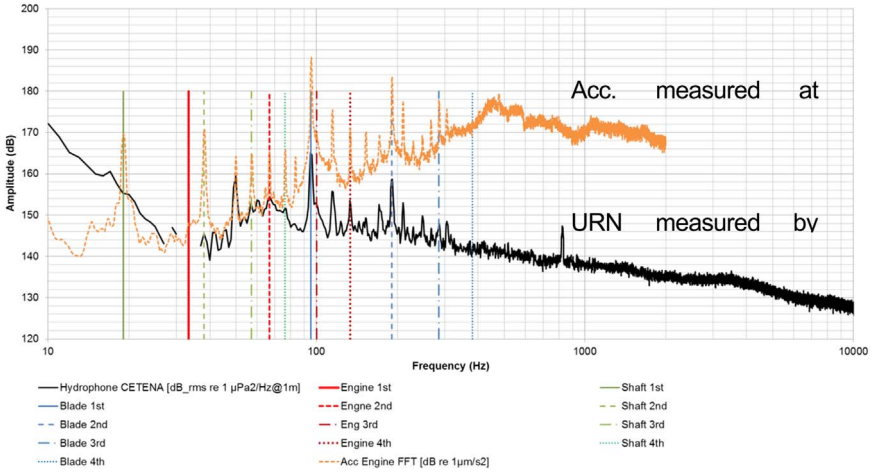

Fig. 13. The narrow band spectrum of the main engine acceleration compared with off-board measurements for 2000 rpm.

noise received SPL and SPL_n is the measured background noise SPL. If the difference was less than 3 dB then the data was discarded.

Measuring the vibration level of the vessel with accelerometers was necessary to identify the noise sources and explore the structural responses as well as to calculate the transmitted energy and structure-borne noise through the structure (Fischer et al., 2008). Vibration level was measured by the accelerometer located near to the pressure sensors, on the port side hull structure and the port side engine foundation. The measurements for the non-cavitating condition (600 rpm engine speed) and heavily cavitating condition (2000 rpm engine speed) are presented in Figs. 12 and 13 to illustrate the effect of the dominant noise sources on the structure in narrow band. At 600 rpm, the vibratory energy of the main engine excites the engine foundation as shown in Fig. 12. In this condition, structure borne noise and background noise are dominating the URN. At 2000 rpm, the cavitating propellers are the dominant noise and vibration sources. Hence, the structural responses of the engine foundation were altered more by cavitation (in the blade passing frequencies) than the main engine (in firing frequencies) as shown in Fig. 13.

To summarize the measurement campaign, the pressure pulses and RNL are proportional to engine speeds (see Figs. 14 and 15). Fig. 16 further shows vessel radiated noise at various engine speeds as well as

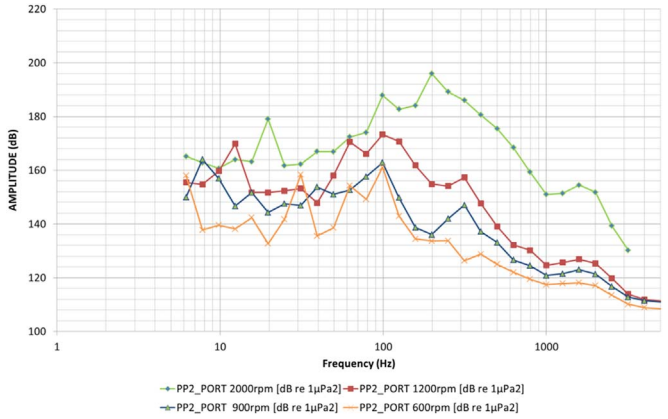

Fig. 14. Pressure pulse spectrum of PP2 for various vessel speed measured by the CETENA on-board.

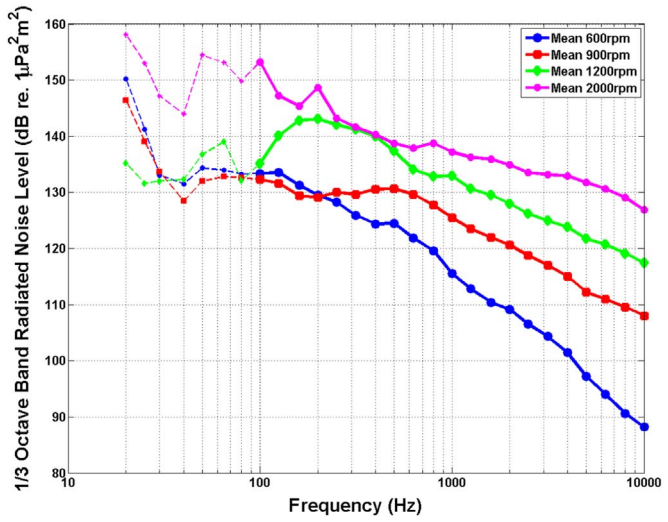

Fig. 15. OTO band radiated noise levels for various engine speed measured on the SOTON off-board hydrophone array (Humphrey and Brooker, 2014).

background (ambient) underwater noise. Background noise seemed to be above the URN when the vessel was operated at the low speeds. This might limit the usability of data from the lower speed runs (SONIC, 2014).

5. Correlation between on-board and off-board measurements

The pressure pulses measured by the pressure sensors were corrected to a 1 m distance based on the cavitation pressure fluctuation prediction formula given in Eq. (3) by Bodger et al. (2014) as shown below. Eq. (3) is established based on two major contributions to the fluctuating hull pressures:

(i) Pressure fluctuations induced by the non-cavitating propeller,
(ii) Those induced by the cavitating propeller, as follows

$$\Delta p_Z = \sqrt{\Delta p_0^2 + \Delta p_C^2 + 2\Delta p_0 \Delta p_c}\ \cos(\pi - \varphi Z) \quad (3)$$

where ΔP_z is the total amplitude of pressure fluctuations, ΔP_0 is the pressure fluctuation due to the non cavitating propeller, ΔP_c is the pressure fluctuation due to the cavitating propeller, φ is the phase angle between the above two components and Z is the blade number.

The calculated correction factors for PP2, PP3 and PP4 for the1 m reference distance is −8.2 dB, −10.3 dB and −3.4 dB respectively. Note that the analysis has concentrated on data from these pressure sensors rather than the accelerometers as they were in direct contact with the water and the pressure corrections were applied for the lower frequencies.

The correlation method is based on the comparison of the radiated noise levels with the pressure pulse levels using graphics as shown Figs. 17–20. A “reference line” was introduced to graphs to show the tendency of the correlation between the pressure sensors and hydrophone more clearly. Two different frequency ranges were selected to evaluate the parameters (RNL and pressure pulse); a lower frequency region (1–500 Hz) and a higher region (1–5 kHz). The correlation in

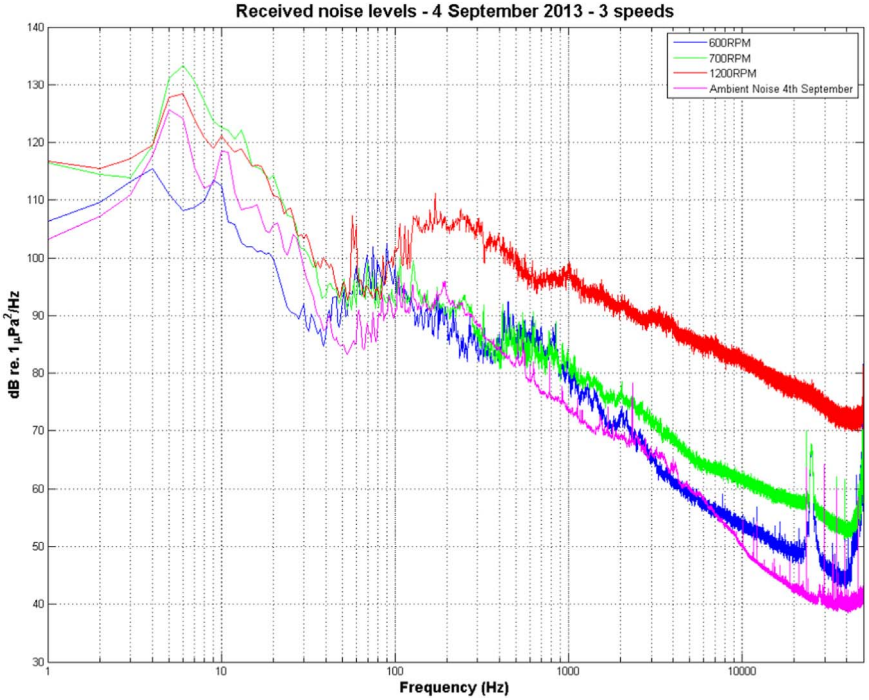

Fig. 16. Received levels of radiated noise from the test vessel compared to levels of background underwater noise in the test area (SONIC, 2014).

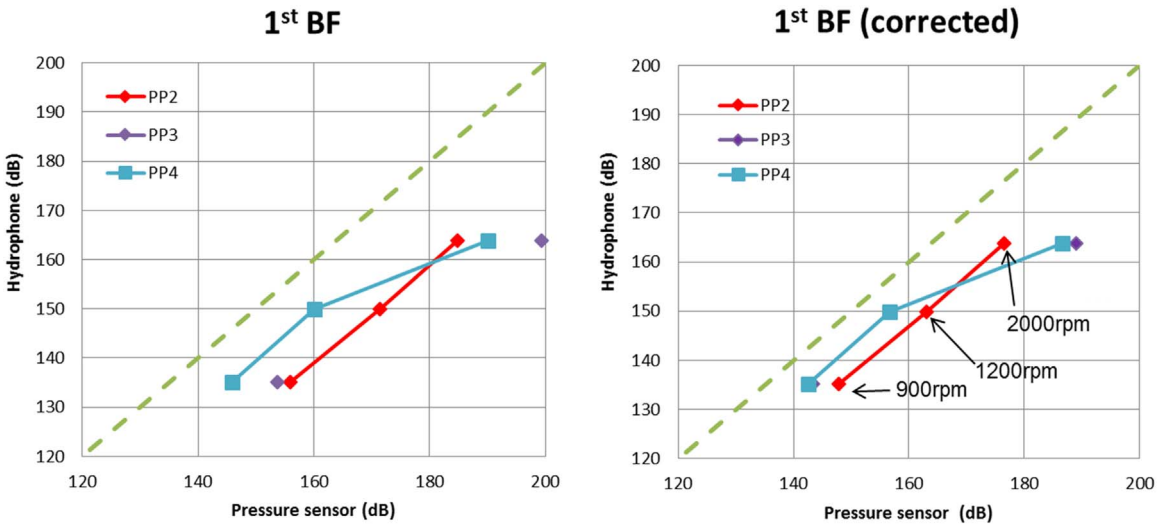

Fig. 17. Correlation between hydrophone RNL and pressure pulse level for 1st blade rate frequency. (Left: not corrected for distance, right: corrected for distance.).

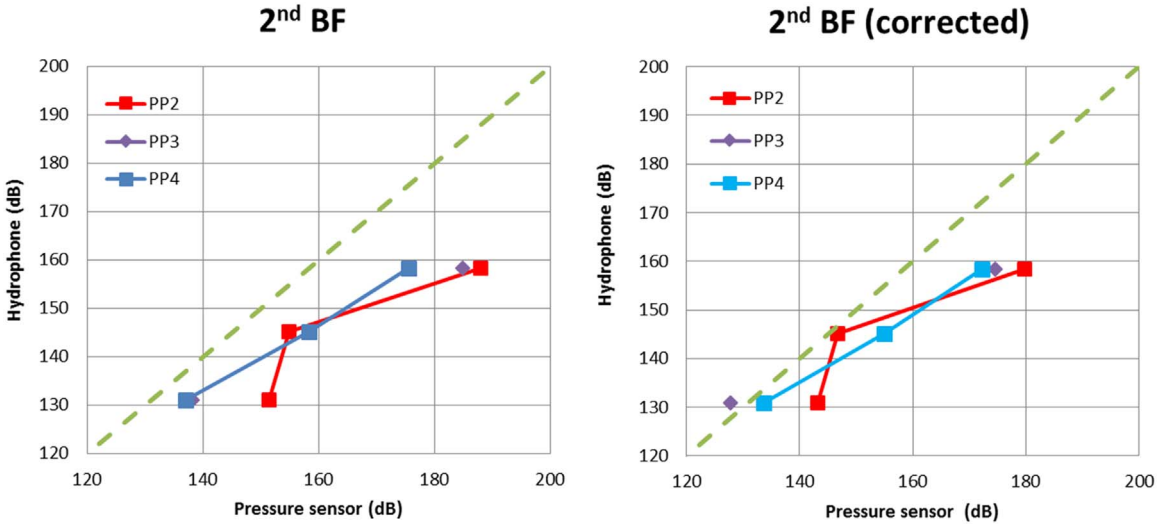

Fig. 18. Correlation between hydrophone RNL and pressure pulse level for 2nd blade rate frequency. (Left: not corrected for distance, right: corrected for distance.).

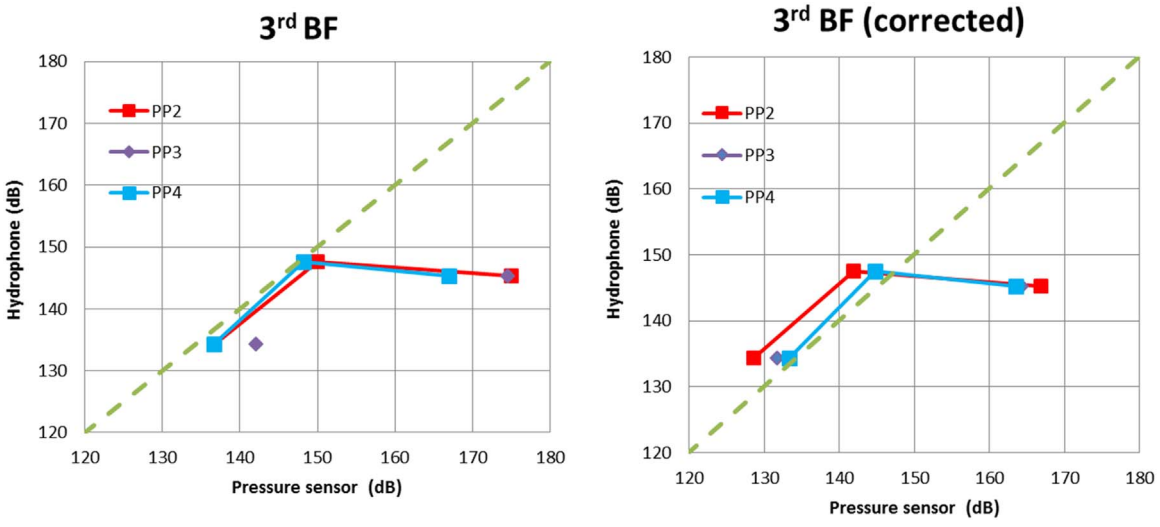

Fig. 19. Correlation between hydrophone RNL and pressure pulse level for 3rd blade rate frequency. (Left: not corrected for distance, right: corrected for distance.).

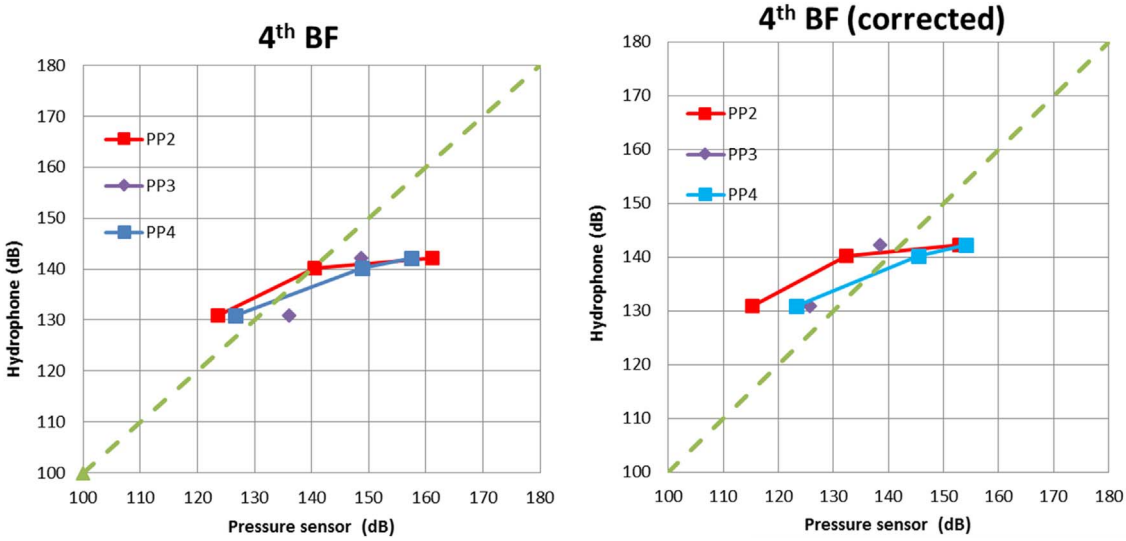

Fig. 20. Correlation between hydrophone RNL and pressure pulse level for 4th blade rate frequency. (Left: not corrected for distance, right: corrected for distance.).

Table. 6–
RNL corresponding to 3rd BPF for each engine speed (Humphrey et al., 2015).

Engine rpm	3BPFs (Hz)	CETENA [dB_rms re 1 $\mu Pa^2/Hz$@1 m]	SOTON [dB_rms re 1 $\mu Pa^2/Hz$@1 m]
900	127	135	134
1200	170	153	147
2000	285	147	145

the high (broadband) frequency region is not presented in this paper as the various noise sources such as unsteady cavitation and turbulent flow are dominating in this region. For this reason, it is difficult to associate tonal noises with the blade passing frequency (BPF) in the URN spectra.

The lower frequency region from 1 Hz to 500 Hz includes the region where the blade passing fundamental and low harmonic frequencies occur. In this region, the amplitudes of the peaks at the BPF seen in the narrow band analyses of the RNL and pressure pulse data recorded for the various engine speeds were extracted.

Derived from the measurements, the curves in Figs. 17 and 18 indicate a clear relationship between the on-board pressure and the off-board radiated noise measurements as engine rpm and hence vessel speed increases. A divergence from this trend is evident at the 3rd BPF shown in Fig. 19. The reason for this divergence is the hydrophone measurement at the 2000 rpm engine speed being lower than 1200 rpm condition at the 3rd BPF, as shown in Table 6. Fig. 20 presents the data for the 4th BPF, which shows a relatively good agreement between the increase in pressure and noise.

6. Conclusion and discussion

In this study traditional as well as innovative methods were employed to obtain URN levels. Results gained from this new correlation method provide insights into the relationship between on-board measured data and URN data. The URN was associated with machinery and ambiance noise before cavitation inception. The structural dynamics were also excited by the main engine. After the cavitation inception, the URN level and pressure pulses were dominated by cavitating propellers. Vibration analysis showed that the structural responses were higher at the blade passing frequencies than at the main engine harmonics when the strong suction side sheet cavitation appeared.

It was experienced that monitoring the measurements in OTO octave band was practical to gain an overall impression of the URN phenomenon, however, narrow band analysis was found to be necessary in order to identify the noise sources accurately. The dominant noise sources were clearly detected in the acceleration data analysed in narrow band. The frequencies at which harmonics of the shafts, the propellers and the main engines occur on the target vessel were very similar and hence could not be easily analysed in OTO band data.

The correlation method presented in this paper is based on the data collected from the pressure sensors and hydrophones. The main reason to concentrate on the pressure sensor data, rather than the accelerometer data, is that both the pressure sensors and hydrophones were operated in the fluid domain and therefore receive the direct transmission of the fluid pressures from the cavitating propellers.

One of the major outcomes from the correlation method is that the radiated noise levels can be associated with pressure sensor data in the low and medium frequency range which covers the first four blade passing frequencies. Underwater radiated noise data can also be obtained with accelerometers and the correlation method can further cover the higher frequency range. Due to the high modal density it is, however, very complicated to associate the results with noise beyond the middle frequency range (~1 kHz). Nevertheless, the accelerometers have an essential role in defining the dominant noise sources on the vessel. The techniques developed in this study can most likely be applied to the determination of URN levels of similar vessels. For this reason, URN levels can be monitored in real time via the deployment of relatively inexpensive equipment.

Acknowledgments

The research, basis for the study made in preparation of this paper, has been supported by the European Union 7th Framework Programme (FP7) project SONIC under grant agreement No: 314394.

References

ANSI, 2004. S1.11-2004, Specification for Octave-band and Fractional-octave-band Analog and Digital Filters, Feb, Standards Secretariat Acoustical Society of America.
ANSI, 2009. Quantities and Procedures for Description and Measurement of Underwater Sound from Ships – Part 1: General Requirements, ANSI/ASA S12.64, American National Standards Institute, New York
Arveson, P., T., Vendittis, D., J., 2000. Radiated noise characteristics of a modern cargo ship. J. Acoust. Soc. Am. 107, 118.
AtlarM., Aktas, B., Sampson, R., Seo, K., C., Viola,M., I., Fitzsimmons, P., Fetherstonhaug, C., 2013, A multi-purpose marine science and technology research vessel for full-scale observations and measurements. In: Proceedings of the 3rd International conference on advanced model measurement technology for the maritime industry (AMT'13), September, Gdansk
Bodger, L., Helma, S., Sasaki, N.2014, Vibration control by propeller design, A. Yucel

Odabasi Symposium In: Proceedings of the 1st International Meeting on Propeller Noise and Vibration, November, Istanbul.
Brooker, A., Humphrey, V. (2014), Measurement of Radiated Underwater Noise from a Small Research Vessel in Shallow Water, A. Yücel Odabaşı Colloquium Series In: Proceedings of the 1st International Meeting - Propeller Noise & Vibration, Istanbul, Turkey
Carlton, J., 2012. Marine Propellers and Propulsion. Butterworth-Heinemann.
Ekinci, S., Celik, F., Guner, M., 2010. A practical noise prediction method for cavitating marine propellers. Brodogradnja 61 (4), 359–366.
Fischer, R., W., Collier, R., D, 2008. Noise Prediction and Prevention on Ships (Handbook of Noise and Vibration Control). John Wiley & Sons, Inc, 1216–1232.
Fischer, R.W., Brown, N.A., 2005. Factors affecting the underwater noise of commercial vessels operating in environmentally sensitive areas. In: Proceedings of OCEANS 2005 MTS/IEEE.
Hallander, J., Göran,B., 2002, Influence of acoustic interaction in noise generating cavitation. In: Proceedings of the 24th Symposium on Naval Hydrodynamics, Fukuoka, Japan, 8-13 July 2002.
Humphrey,V., Brooker, A., Dambra, R., Firenze, E., 2015. Variability of Underwater Radiated Ship Noise Measured Using Two Hydrophone Arrays, OCEANS 2015-Genova, IEEE.
Humphrey, V., Brooker, A., 2014, Measurement of Radiated Underwater Noise from a Small Research Vessel in Shallow Water, A. Yucel Odabasi Symposium In: Proceedings of the 1st International Meeting on Propeller Noise and Vibration, November, Istanbul.
ISO/PAS, 2012. 17028-1. Acoustics – Quantities and procedures for description and measurement of underwater sound from ships Part 1: General requirements for measurements in deep water, ISO, Geneva.
ITTC, 2014. Specialist Committee on Hydrodynamic Noise. In: Final Report and Recommendations to the 27th ITTC (p. 45). Copenhagen, Sweden.
Kinnas, S.A., Lee, H., Young, Y.L., 2003. Modeling of unsteady sheet cavitation on marine propeller blades. Int. J. Rotating Mach. 9 (4), 263–277.
Nilsson, S., Tyvand, N.P., 1981. Noise Sources in Ships: I Propellers, II Diesel Engines, Nordic Cooperative Project: Structure Borne Sound in Ships from Propellers and Diesel Engines, Nordforsk, Norway.
Sampson, R., Turkmen, S., Aktas, B., Shi, W., Fitzsimmons, P., Atlar, M., 2015. On the full scale and model scale cavitation comparisons of a Deep-V catamaran research vessel. In: Proceedings of the 4th International Symposium on Marine Propulsors (SMP'15), Austin, Texas. June.
Sasajima, T., Nakamura, Oshima, A., 1986. Model and full scale measurements of propeller cavitation noise on an oceanographic research ship with two different types of screw propeller. In: Bulletin, J. (Ed.), Shipboard Acoustics(ed). Martinus Nijhoff Publishers, Dordrecht, Netherlands.
SONIC, 2012. Suppression of underwater Noise Induced by Cavitation, Annex-I Description of Work, EU-FP7 Collaborative project, Grant agreement no: 314394.
SONIC, 2014. Suppression of underwater Noise Induced by Cavitation, WP2-1st Periodic Report.
Szantyr, J.A., 1985. A new method for the analysis of Un-steady Propeller cavitation and hull surface pressures. R. Inst. Nav. Archit., 127, 153–163, (1984).
Urick, R.J., 1967. Principles of Underwater Sound for Supervisors. McGraw-Hill, New York.
Vorus, W.S., 1988. VibrationPrinciples of Naval Architecture Vol II. SNAME.
Wales, S., C., Heitmeyer, R., M., 2002. An ensemble source spectra model for merchant ship-radiated noise. J. Acoust. Soc. Am. 111 (3), 1211–1231.
Wenz, G., 1962. Acoustic ambient noise in the ocean: spectra and sources. J. Acoust. Soc. Am. 34, 1936.